Check for updates

RESEARCH ARTICLE

NANO · MICRO small
www.small-journal.com

Nasal Delivery of mRNA Using Thermoresponsive Gellable Aqueous Biphasic Systems

*Bojan Kopilovic, Nabila Laroui, João A.P. Coutinho, Chantal Pichon, and Mara G. Freire**

Messenger ribonucleic acid (mRNA) emerged as a versatile therapeutic for the prevention and treatment of various diseases, being widely used in the "third-generation vaccines." Innovative delivery vehicles, including lipid nanoparticles and liposomes, were developed to preserve mRNA and allow efficient delivery. On the other hand, nasal vaccination has demonstrated to be effective against respiratory infections. Nevertheless, mRNA's vulnerability to enzymatic degradation, low nasal permeability, and rapid clearance are still critical challenges. Liposomal hydrogels enable bioadhesion and localized drug release; however, these may exhibit cytotoxicity due to the required cross-linking agents. To overcome these drawbacks, a gellable aqueous biphasic system (ABS), composed of water, poly(ethylene) glycol, and gelatin is proposed, as a promising approach for mRNA nasal delivery. This approach, using a gellable biopolymer, eliminates the need for chemical cross-linkers. The developed liposomal hydrogels enables localized and safe mRNA release without associated cytotoxicity toward upper airway epithelial cells. Validation through scanning electron and fluorescence microscopies reveal efficient mRNA entrapment, with a prolonged delivery of up to 30 min. Additionally, by entrapping nanoparticles within hydrogels, a significant reduction in toxicity is demonstrated. The formulated liposomal hydrogels demonstrate comparable transfection efficiency to commercial alternatives, showcasing their potential for safe and effective nasal gene delivery.

1. Introduction

Modulating protein expression offers a powerful approach to prevent and treat a wide range of diseases. While protein therapeutics hold promise, their direct clinical application is often hindered by high production costs, instability, and challenges in achieving effective in vivo concentrations.[1] Accordingly, alternative strategies have been investigated, including gene-based therapies that employ messenger ribonucleic acid (mRNA) to introduce therapeutic genes into target cells.[2,3] Among the several available gene-based therapies, mRNA has attracted extensive interest from researchers and biopharmaceutical companies.[4–6] mRNA offers several advantages over other gene-based therapeutics, including a low risk of genomic mutagenesis, natural degradation through cellular pathways, and the ability to bypass nuclear membrane transport. Additionally, it enables transient and rapid protein expression in the cell cytoplasm, making it a promising candidate for the development of antiviral and anti-tumor vaccines.[4,6–8] However, naked or free mRNA is easily degraded by RNase and cannot pass through the cell membrane.[8] Therefore, a delivery vehicle is required to transport mRNA into cells and express the coded protein.

Vaccine development has been accelerated with the production of high-quality nucleic acids using in vitro transcribed messenger ribonucleic acid (IVT-mRNA), commonly described as "third-generation vaccines."[8] These advances also facilitated the development of delivery vehicles, including lipid nanoparticles, liposomes, lipoplexes, and lipopolyplexes, which play a crucial role in the endocytosis and stability preservation of the gene delivery agent – mRNA.[5,6]

B. Kopilovic, J. A. Coutinho, M. G. Freire
CICECO – Aveiro Institute of Materials
Department of Chemistry
University of Aveiro
Aveiro 3810-193, Portugal
E-mail: maragfreire@ua.pt

The ORCID identification number(s) for the author(s) of this article can be found under https://doi.org/10.1002/smll.202409527

© 2025 The Author(s). Small published by Wiley-VCH GmbH. This is an open access article under the terms of the Creative Commons Attribution-NonCommercial-NoDerivs License, which permits use and distribution in any medium, provided the original work is properly cited, the use is non-commercial and no modifications or adaptations are made.

DOI: 10.1002/smll.202409527

N. Laroui, C. Pichon
Centre de Biophysique Moléculaire (CBM)
UPR 4301 CNRS
University of Orléans
Orléans F-45071, France

N. Laroui, C. Pichon
ART ARNm Inserm UMS 55 and LI2RSO-University of Orléans
Orléans F-45100, France

N. Laroui, C. Pichon
Institut Universitaire de France
1 rue Descartes, Paris F-75035, France

Vaccines delivered via the conventional intramuscular route predominantly induce a systemic immune response, by the production of serum immunoglobulin G (IgG) antibodies. Nevertheless, this approach typically does not provoke a significant mucosal immune response that allows an effective memory immune response.[2] This drawback can be overcome by the nasal administration of vaccines, being shown to be an effective approach to tackle respiratory infections, including those derived from SARS-CoV-2 and respiratory syncytial virus and influenza.[9,10] This route of vaccination offers the advantage of producing secretory immunoglobulin A antibodies, which block pathogens in mucus during early infection stages while generating long-lasting resident memory T cells in mucosal tissues for future protection.[2] Mucosal administration of nucleic acid vaccines to sites such as the nasal and pulmonary mucosa enables them to reach draining mucosal lymph nodes via the lymphatic systems underlying the airway epithelium.[9,11]

Despite their relevance, effective nasal delivery strategies are still required due to the delicate nature of mRNA, which is vulnerable to degradation, exhibits low permeability across the nasal epithelium, and is rapidly cleared from the nasal mucosa.[2,12] The causes of stability loss are often related to the process conditions and may include extreme temperatures and pH values, or the presence of organic solvents, often required in encapsulation strategies.[13,14] As a result of instability, the immunogenicity of aggregated or degraded mRNA is becoming increasingly important, being essential to develop stable and effective formulations for nasal delivery.[15,16]

The efficacy of liposomal drug delivery systems has been debated due to their potential for accumulation in healthy tissues upon intravenous administration, leading to adverse side effects and reduced therapeutic outcomes.[17] Nonetheless, a promising solution has emerged through the integration of liposomes into hydrogel matrices, which not only enhance the mechanical attributes of liposome formulations but also enable a localized and sustained drug release.[18] These hydrogels are usually prepared using polymers, providing a robust platform for innovative therapeutic approaches.[7,19] Natural stimuli-responsive biomaterials, such as gelatin, are often studied for drug delivery and tissue engineering due to their high biocompatibility and adjustable mechanical properties.[20] Gelatin provides integrin-binding arginylglycylaspartic acid motifs and metalloprotease cleavage sites, which facilitate tissue adhesion and integration.[21] Furthermore, gelatin hydrogels can swell and hold a large amount of water while maintaining their structure. This property allows for the controlled release of bioactive molecules.[20]

Schwabe et al.[22] developed a gelatin hydrogel loaded with lipopolyplexes to control the release of small interfering RNA (siRNA).[22] In this work, oligomeric cross-linkers were used to tailor the properties of the hydrogels, with the cross-linking density of the hydrogel influencing the rate of the siRNA release. Similarly, Furst et al.[23] incorporated poly(ethylene) glycol (PEG)-modified lipoplexes into hydrogels prepared of hydroxyethyl cellulose for the target delivery of siRNA to the vaginal mucosa. Chen et al.,[24] on the other hand, developed scaffolds and studied transfection efficiencies using (green fluorescent protein) GFP-mRNA lipoplexes-loaded hydrogel systems. These scaffolds were implanted in animals, demonstrating that the loaded hydrogels outperformed both naked mRNA delivery from the scaffolds and subcutaneous injections of lipoplexes. Despite the promising results, some prepared hydrogels resorted to the use of cross-linking agents, which may raise cytotoxicity concerns.[25] Some of these studies did not incorporate bio-derived cross-linkers, which could enhance both sustainability and reduce toxicity, nor did focus on the development of simple, ready-to-use hydrogels to improve clinical feasibility.

To ensure biocompatibility and to minimize the use of potentially harmful cross-linkers, herein we propose a novel strategy based on gellable aqueous biphasic systems (ABS).[21] ABS are here used to create hydrogels, with one of the ABS components being stimuli-sensitive leading to gel formation, while mimicking the characteristics of a water-in-water (W/W) emulsion. Despite their relevance, ABS composed of non-gellable polymers have been majorly investigatedas liquid–liquid systems to purify biomolecules,[26] including biopharmaceuticals.[27,28] Gellable ABS reported herein are composed of water, poly(ethylene) glycol, and gelatin as the gellable polymer, allowing to have thermoresponsive ABS in which changes from liquid–liquid to gel-liquid systems occur by changes in temperature. The components for these systems were chosen based on their innate biocompatibility and ability to interact well with mRNA-carrying vehicles. These interactions are critical for successfully entrapping mRNA delivery vehicles within the hydrogel matrix. Furthermore, in nasal formulation development, increased quantities of PEGylated lipids or PEG polymers are a frequent method to improve particle transition through the mucosa.[29] These compounds were carefully selected to additionally offer tissue bio adhesivity, invisibility to the immune system, and prolonged drug delivery. The studied thermoresponsive ABS can be tailored to produce microspheres or block hydrogel shapes, effectively functioning as reservoir systems, enclosing mRNA-loaded liposomes within their matrices. By finely tuning the formulation parameters such as component concentration, PEG molecular weight, mixing speed, and temperature, we controlled the phase separation process, resulting in different sphere sizes and hydrogels with distinct characteristics. In comparison to reported literature,[22–24] we avoid the use of cross-linkers to improve biodegradability and reduce health and environmental risks by employing a gellable biopolymer. Moreover, the developed one-pot or ready-to-use hydrogel system simplifies the overall preparation process and facilitates usability, while offering a prolonged alternative for nasal delivery. The developed hydrogels exhibited controlled degradation rates while maintaining biopharmaceutical stability. In summary, the studied hydrogels demonstrated efficient mRNA delivery, with negligible cytotoxicity and effective therapeutic efficacy in upper airway epithelial cells.

2. Results and Discussion

2.1. Gellable ABS Preparation and Characterization

Figure 1 shows the workflow of mRNA-loaded liposome hydrogel formulation, characterization, and application. It highlights key steps, including the formation of gellable ABS, its thermoresponsive properties, and its potential for controlled drug delivery. Specifically, Figure 1A depicts the formulation and optimization

© 2025 The Author(s). Small published by Wiley-VCH GmbH

16136829, 0, Downloaded from https://onlinelibrary.wiley.com/doi/10.1002/smll.202409527 by Universidade De Aveiro, Wiley Online Library on [24/02/2025]. See the Terms and Conditions (https://onlinelibrary.wiley.com/terms-and-conditions) on Wiley Online Library for rules of use; OA articles are governed by the applicable Creative Commons License

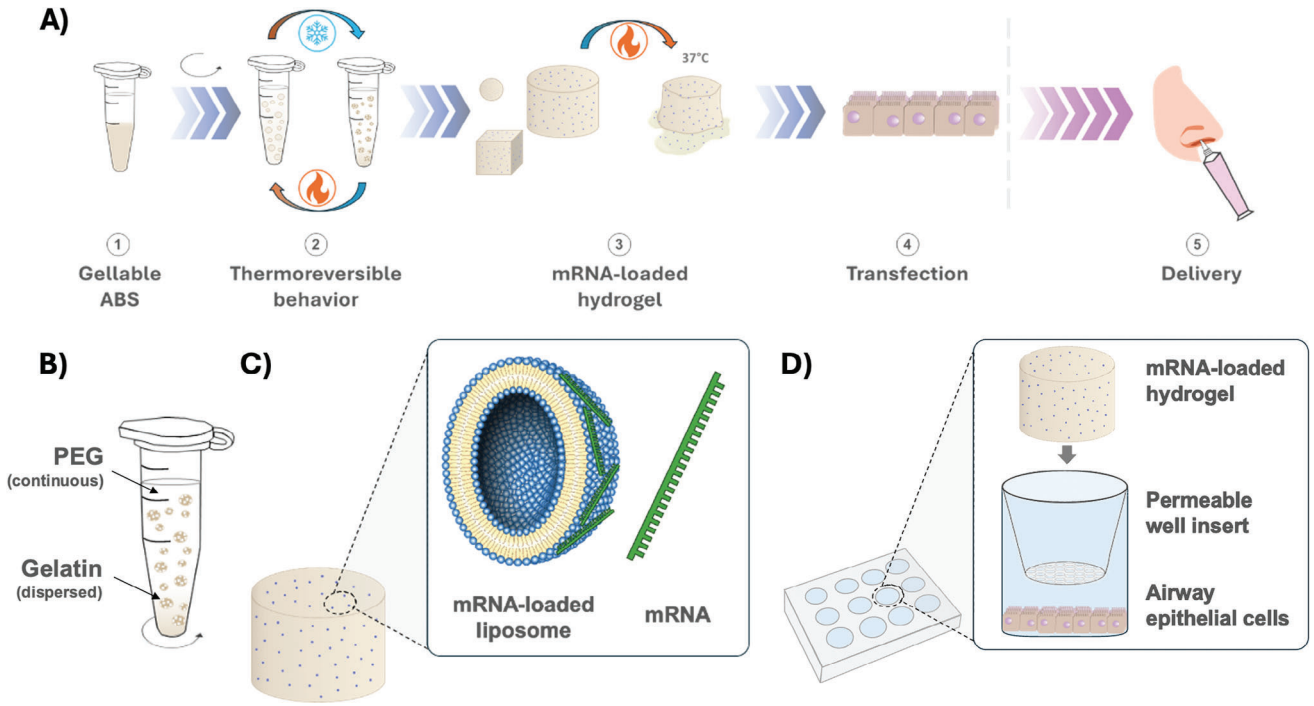

Figure 1. Preparation and characterization workflow of mRNA-loaded liposome hydrogel. A) Formulation of gellable ABS as hydrogels, including future delivery perspectives. Illustration of the thermoresponsive behavior of engineered ABS implemented in hydrogel formulation. B) Gellable ABS composition. C) Representation of mRNA-loaded liposomes within the hydrogel matrix. D) Representation of the upper airway epithelial cell transfection assays with mRNA-loaded liposome hydrogels.

process for developing ABS as hydrogels of adaptable shapes, while Figure 1B identifies the ABS continuous and dispersed phases. Figure 1C shows the mRNA-loaded liposomes entrapped within the hydrogel matrix, being crucial for the stability maintenance and controlled release of mRNA. Figure 1D presents how the transfection assays on upper airway epithelial cells covered in mucin were performed, allowing to address the cytocompatibility of the mRNA-loaded hydrogels and their delivery efficacy.

Understanding and optimizing ABS ensures that the resulting delivery devices possess the desired characteristics for effective mRNA delivery. Accordingly, the phase diagrams for the gellable ABS composed of water, gelatin, and PEG of different molecular weights (2 000, 4 000, 6 000, 8 000, 10 000, and 20 000 g mol^{-1}) were determined at 40 °C, a temperature at which the gelatin is soluble in water (the gelation temperature of the used gelatin is 32 °C).[30] The obtained phase diagrams, in which the binodal curves separating the monophasic from the biphasic regime are provided, are given in Tables S1,S2 and Figure S1 (Supporting Information). In general, the liquid–liquid demixing ability increases with the increase of the PEG molecular weight. This trend is justified by the higher hydrophobicity of PEGs with longer alkyl chains, requiring lower amounts of gelatin to undergo phase separation. The obtained phase diagrams, illustrated in Figure S1 (Supporting Information), are in close agreement with some that have been previously reported.[31]

With the previously discussed data on the ABS phase diagrams, we then carefully selected appropriate mixture points to enhance the overall biocompatibility of the aimed mRNA delivery platform, particularly by increasing the water content and decreasing the PEG and gelatin concentrations. Lower PEG concentrations reduce the likelihood of cytotoxicity associated with high PEG concentrations,[32] while reducing gelatin concentration can minimize the potential for adverse immune reactions, thereby improving the biocompatibility of the system.[33] Hydrogels or microspheres can be formed at temperatures below the gelation temperature of gelatin, resulting from the reorganization of random coil structures into helices stabilized by hydrogen bonds established between the amino acid residues of adjacent chains.[34]

Gelatin-rich microsphere creation was first attempted under continuous mixing of the gellable ABS for 15 min, followed by a 5 min period of mixing with the sample placed over an ice water bath (4 °C), which due to the immiscibility of the phases results in the formation of gelatin-rich spheres in a continuous PEG-rich phase. For the preparation of hydrogels, an additional centrifugation step at 4 °C was then performed. The gelatin microsphere size was evaluated by varying different parameters, namely the PEG molecular weight, temperature, and mixing speed. The average size of the obtained microspheres (in ethanol 95% (v/v) to prevent swelling) for each set of mixing speeds and PEG molecular weights is shown in **Figure 2**, while the histograms of the respective microspheres are presented in Figure S2 (Supporting Information). The temperature influence on the microsphere size is shown in Figure 2B, provided in Supporting Information). In general, the mixing speed and PEG molecular weight have a significant impact on the microsphere size, with average sizes ranging from 2 to 34 µm. The average microsphere size increases as the mixing speed increases, in

© 2025 The Author(s). Small published by Wiley-VCH GmbH

16136829, 0, Downloaded from https://onlinelibrary.wiley.com/doi/10.1002/smll.202409527 by Universidade De Aveiro, Wiley Online Library on [24/02/2025]. See the Terms and Conditions (https://onlinelibrary.wiley.com/terms-and-conditions) on Wiley Online Library for rules of use; OA articles are governed by the applicable Creative Commons License

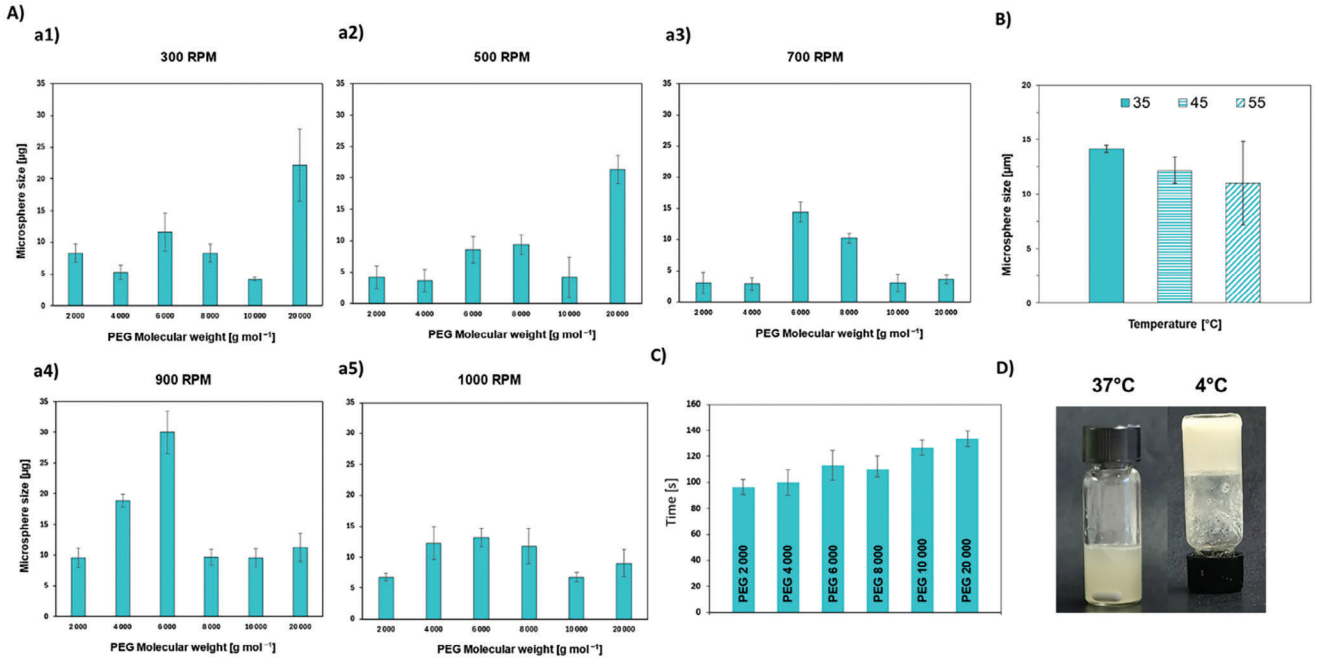

Figure 2. Characterization of gellable ABS. A) Influence of the PEG molecular weight on the size of gelatin microspheres produced from 5 wt.% gelatin + 10 wt.% PEG ABS at 40 °C and various mixing speeds – measured using ImageJ software. B) Influence of temperature on the size of gelatin microspheres produced from 5 wt.% gelatin + 10 wt.% PEG 20 000 at 500 RPM – measured using ImageJ software. C) Gelation time of the gellable ABS produced from 5 wt.% gelatin + 10 wt.% PEG, verified by the D) Inverted tube test of the gelatin-rich hydrogel.

accordance with previous studies.[31] However, this trend was not visible in the most viscous system containing PEG 20 000, meaning that the high-viscous systems cannot be tailored in this regard. A similar phenomenon was observed previously by Butler et al.,[35] who noticed higher droplet coalescence at lower shear rates and attributed this to be the cause of the accelerated coarsening of gelatin microspheres.[35] These trends are also supported by (Figure S2, Supporting Information) the observed polydispersity increase in the less viscous systems with the increase in the mixing speeds. On the other hand, a mixing speed of 700 RPM consistently produced the smallest microspheres in all studied systems. However, it should be noted that a particle size analyzer should be used to confirm the hydrodynamic radius of the obtained microspheres.

Figures 2B and S2B (Supporting Information) illustrate the influence of temperature in modulating the microsphere size within the PEG 20 000 + gelatin ABS. Overall, the higher the temperature, the lower the microsphere size. This trend is due to the reduction in the viscosity of the emulsified phase at higher temperatures. As observed by Butler et al.,[35] droplet coalescence becomes more pronounced at higher temperatures due to the lower viscosity of the system, explaining the larger error bar observed for the system at 55 °C in Figure 2B.

As previously highlighted, gelatin also enables hydrogel formation by changes in temperature, thus not requiring the addition of cross-linkers or other compounds. Figure 2D shows the inverted tube test of a system containing 5 wt.% gelatin + 10 wt.% PEG 20 000 + 85 wt.% water, whereas Figure 2C illustrates the influence of the PEG molecular weight on the gelation time of the studied system following the inverted tube test. It is evident that as the molecular size of PEG increases, the time required for the hydrogel formation also increases. As we have a gelatin-rich phase also comprising some PEG, this trend may result from steric effects, with the PEG molecular weight influencing the gelatin's ability to form a helical structure.

To confirm the presence of spheres in the gelatin-rich phase in the hydrogel form, the hydrogel and its cross-section morphology were evaluated by scanning electron microscopy (SEM) using chosen emulsification conditions. **Figure 3** shows that gelatin microspheres are large non-homogeneous polymeric structures with a porous morphology, retained in a PEG matrix (Figure 3A1), consisting of a cluster of several interconnected spherical gelatin particles (Figure 3A2) typical of gelatin structures.[36,37] Figure 3-A3,A4 represent cross-sections of the prepared hydrogels, where the hollow middle and porous particle wall structure of the gelatin microspheres can be confirmed.[36,37] The size of the gelatin spheres in the hydrogel is generally consistent with the microscopic measurements, though they may be slightly larger than those determined by microscopy. This discrepancy can be attributed to differences in the SEM sample preparation method, as the hydrogel preparation process likely leads to sphere coalescence during centrifugation, resulting in spheres of up to 100 µm.

2.2. Characterization of the mRNA-Carrying Liposomes Loaded in the Gellable ABS

As summarized in Figure 1, after developing and characterizing the gellable ABS, mRNA-loaded liposomes were loaded into the

© 2025 The Author(s). Small published by Wiley-VCH GmbH

16136829, 0, Downloaded from https://onlinelibrary.wiley.com/doi/10.1002/smll.202409527 by Universidade De Aveiro, Wiley Online Library on [24/02/2025]. See the Terms and Conditions (https://onlinelibrary.wiley.com/terms-and-conditions) on Wiley Online Library for rules of use; OA articles are governed by the applicable Creative Commons License

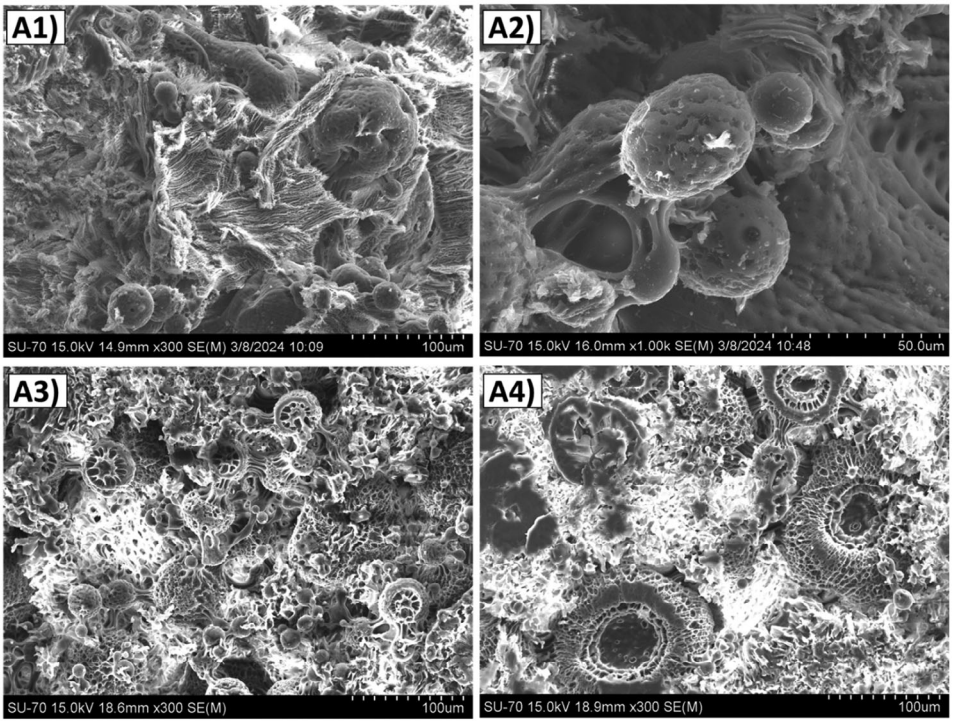

Figure 3. SEM images showing the dispersed gelatin-rich ABS phase corresponding to the obtained hydrogels A1,A2) and their cross-section views A3,A4). Gelatin-rich hydrogels were produced from 5 wt.% gelatin + 10 wt.% PEG + 85 wt.% water.

hydrogel matrix. The successfully loaded hydrogels were characterized through fluorescence microscopy, fluorimetry, and hydrogel degradation assays. Additionally, the mRNA delivery performance was assessed using upper airway epithelial cells, the studied cell line for nasal delivery.

The gene delivery performance of the developed gellable system was addressed by using lipoplexes containing mRNA encapsulated by liposomes – commercial Lipofectamine (LFM) and an in-house prepared liposome (lip).[38] **Figure** 4A,B shows brightfield and fluorescent microscopic images of gelatin microspheres and a liposome-loaded hydrogel containing gelatin microspheres, respectively, formed using an ABS comprised of 5 wt.% gelatin + 10 wt.% PEG 20 000 + 85 wt.% water. This system contained liposomes complexed with fluorescein isothiocyanate (FITC)-labeled mRNA, enabling the visualization of the gene delivery cargo as bright green spots. Since gelatin slightly interfered with the fluorescent microscopy imaging, evident as faded green spheres in the background, additional fluorometric experiments of the loaded microspheres were performed at λ_{ex} = 495 nm and λ_{em} = 520 nm. At the specific excitation and emission wavelengths of FITC, the influence of gelatin is less significant (Figure 4C).

The drug carrier degradability is a crucial factor influencing the effectiveness, safety, and long-term therapeutic outcome. The degradation rate of the gelatin-based hydrogels was studied in PBS at 37 °C, with samples collected at various time points (1 to 60 min), followed by protein quantification. The observed degradation of the gelatin-rich hydrogel above its gelling temperature (32 °C) results in the gradual disruption of the gelatin helical matrix, enabling the controlled release of mRNA-carrying vehicles. As shown in Figure 4D, the developed hydrogels ensure prolonged contact with mucosal surfaces, with the complete hydrogel degradation occurring after 30 min, and therefore having the potential to resist mucociliary clearance. This resistance to clearance not only enhances drug delivery but also optimizes therapeutic effectiveness. Moreover, to ensure the stability of the gelatin hydrogel during storage, it is recommended to maintain conditions below its gelation temperature, preferably in a cold environment, and using its hydrogel form and not an aqueous solution.

The successful loading of anti-reverse cap analog (ARCA)-capped GFP mRNA at RNA/liposome charge ratio of 1:1.5 within the gelatin microspheres is confirmed by the results shown in Figure 4E, while also proving the stability of the mRNA after gelation and release. In phosphate buffer, liposomes containing an ionizable lipid have a minor positive charge, while mRNA exhibits a slight negative charge due to its phosphate group backbone. This difference in charge polarities facilitates the association and complexation of the positively charged liposomes with the negatively charged mRNA. This electrostatically ruled environment extends to the gelatin microspheres, which possess a slight negative charge within the range of pH 6 to 9.4 (isoelectric point, pI).[39] Consequently, the microspheres attract and interact with the positively charged liposomes, further enhancing the loading of the mRNA visible as a dark band in Figure 4E. However, the interaction of mRNA and gelatin should not be entirely ruled out. Moreover, it is evident that the mRNA is preferentially partitioned to the gelatin-rich phase and is stable even after release.

© 2025 The Author(s). Small published by Wiley-VCH GmbH

16136829, 0, Downloaded from https://onlinelibrary.wiley.com/doi/10.1002/smll.202409527 by Universidade De Aveiro, Wiley Online Library on [24/02/2025]. See the Terms and Conditions (https://onlinelibrary.wiley.com/terms-and-conditions) on Wiley Online Library for rules of use; OA articles are governed by the applicable Creative Commons License

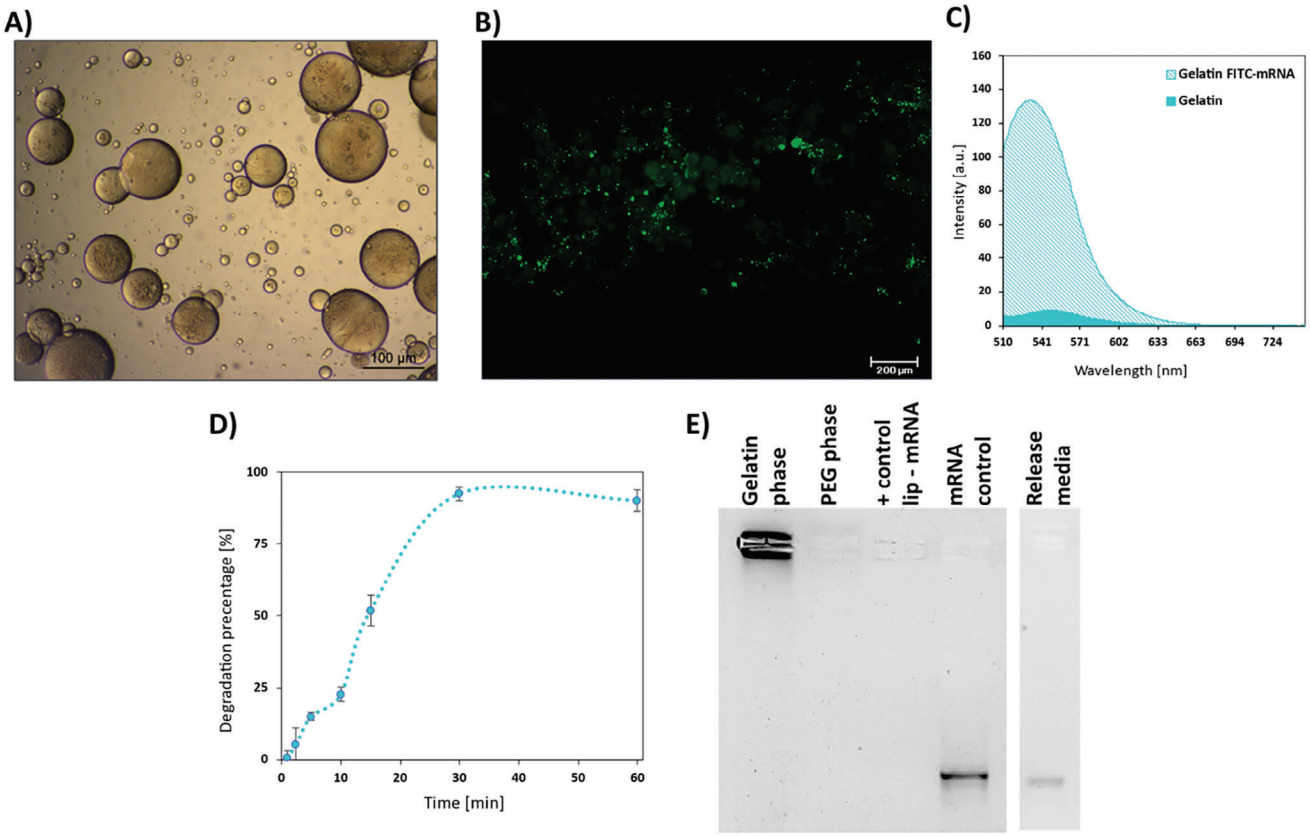

Figure 4. Characterization and biological evaluation of the mRNA-loaded gelatin-rich hydrogel comprising 5 wt.% gelatin + 10 wt.% PEG 20 000 + 85 wt.% water. A) Fluorescent microscopic image (20 × magnification) of gelatin microspheres entrapping FITC-labelled mRNA. The gelatin microspheres comprised 0.1 wv% FITC-mRNA, enabling the visualization of the gene delivery cargo as bright green spots. B) Fluorescence spectra of gelatin microspheres and FITC-mRNA-loaded microspheres in an aqueous solution of pH = 7.4 at 37 °C. C) The degradation profile of the gelatin-rich hydrogel studied in PBS at 37 °C, up to 60 min, obtained by protein quantification assay. D) Evaluation of lipoplex formation and partitioning by agarose gel electrophoresis. mRNA complexation: all samples were prepared comprising 200 ng of mRNA, except the hydrogel loaded with lipoplex which contained 500 ng of mRNA, at RNA/liposome charge ratio of 1:1.5. Positive control was the studied lipoplex.

2.3. Biological Evaluation of the mRNA-Carrying Liposomes Loaded in the Gellable ABS

As shown earlier, the gellable ABS containing anti-reverse cap analog (ARCA)-capped mRNA-loaded liposomes is thermoreversible. Thus, when exposed to temperatures exceeding the gelation temperature of gelatin (above 32 °C), the hydrogel undergoes a conformational change, leading to the loss of its helical structure and the disintegration of the gel network. This disruption of the hydrogel matrix results in the controlled release of mRNA-carrying liposomes, as the electrostatic interactions between gelatin and the liposomes weaken, allowing the mRNA-loaded vehicles to be released from the matrix into the surrounding environment. To evaluate the ability of the developed hydrogel to deliver mRNA into cells and express encoded proteins, hydrogel loaded with GFP mRNA was delivered to human upper airway epithelial cells covered in a mucin layer.

The encapsulation efficiency of mRNA within the liposomes was determined to be 89.9%, by the Ribogreen assay. **Figure** 5A displays the survival rate of H292 cells, measured 24 h after mRNA delivery. The survival rate of the cells was assessed using flow cytometry, to evaluate the cytotoxicity of the conventional and proposed gelatin-based hydrogel delivery systems (Figure 5A). The results indicate that the gelatin-based hydrogels delivering mRNA in LFM and lip exhibit minimal cytotoxicity – 96% and 97% of cell viability, respectively.

Overall, these findings emphasize the safety advantages of utilizing the gelatin-rich hydrogel, making it a promising candidate for applications involving nasal delivery. Furthermore, a successful delivery of the genetic material required for protein production was achieved within the studied cell line, enabling the expression of GFP (Figure 5B). In terms of cell transfection, the results show that both LFM and lip entrapped in the hydrogel have similar levels of cell transfection (66% and 60%, respectively). However, the transfection efficiency of the lipoplexes released from the hydrogel is lower compared to the conventionally delivered LFM and liposome formulations, with the same applying to the mean fluorescence intensity (MFI) of the expressed GFP. Still, the developed delivery platform exhibits remarkable cytocompatibility and effective cell transfection, while showing favorable GFP expression in the case of the commercial formulation (LFM). The developed hydrogels formed by gellable ABS

© 2025 The Author(s). Small published by Wiley-VCH GmbH

16136829, 0, Downloaded from https://onlinelibrary.wiley.com/doi/10.1002/smll.202409527 by Universidade De Aveiro, Wiley Online Library on [24/02/2025]. See the Terms and Conditions (https://onlinelibrary.wiley.com/terms-and-conditions) on Wiley Online Library for rules of use; OA articles are governed by the applicable Creative Commons License

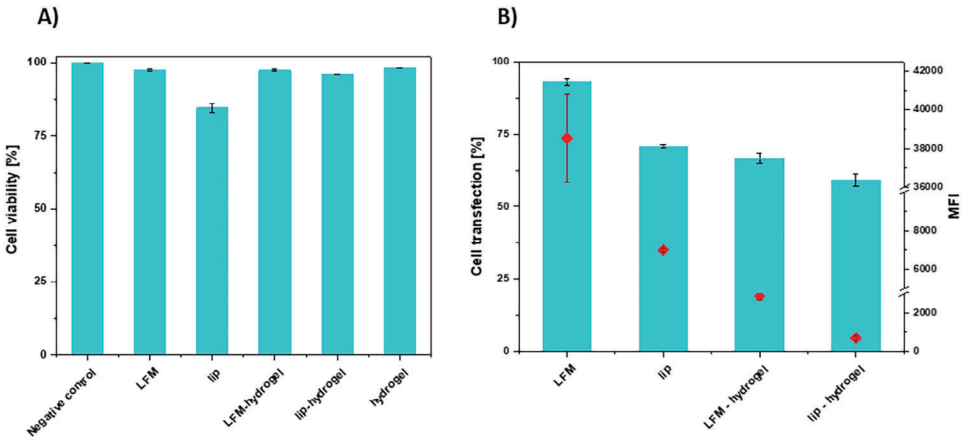

Figure 5. Biological evaluation of the mRNA-loaded gelatin-rich hydrogel comprising 5 wt.% gelatin + 10 wt.% PEG 20 000 + 85 wt.% water. A) Viability of H292 upper airway epithelial cells 24 h after mRNA-loaded hydrogel exposure. Hydrogels were prepared with commercial lipofectamine and in-house liposome formulations containing 0.5 μg of anti-reverse cap analog (ARCA)-capped mRNA at an RNA/liposome charge ratio of 1:1.5. B) Percentage of cell transfection (bars) and mean fluorescence intensity (MFI) (scatter chart) were measured 24 h after treatment of cells with lipoplexes comprising 0.5 μg of mRNA at an RNA/liposome charge ratio of 1:1.5. Data are expressed as percentage of GFP positive cells. Data are presented as mean ± SD of experiments performed in triplicates ($n = 3$).

have strong potential for achieving high protein expression and expanding therapeutic applications, opening the door to a safer mRNA nasal delivery platform. However, it should be remarked that the performance of these systems can be influenced by the properties of gelatin, such as gelling strength, melting point, and allergenicity, which vary depending on the gelatin source.

3. Conclusions

Conventional needle-based mRNA delivery methods often face limitations, including safety concerns, pain, and the requirement of trained professionals, in addition to logistical challenges such as the need for cold chain storage. To overcome these challenges, we developed a novel approach for mRNA delivery, via nasal delivery using gelatin-based thermoresponsive ABS. These gellable systems, composed of gelatin, PEG, and water have the ability to modulate hydrogel properties through variations in formulation parameters, allowing to tailor drug delivery profiles. With minimal cytotoxicity toward upper airway epithelial cells, transfection efficiency of 60%, prolonged mRNA release (up to 30 min), and noninvasivenoninvasive route of administration, gelatin-based thermoresponsive ABS holds high potential in the field of mRNA delivery. Future studies should focus on evaluating the therapeutic efficacy and safety of the ABS system through in vivo experiments to further validate its potential for clinical applications. With the potential for further optimization, including improved protein expression and targeted delivery, gellable ABS show promise for advancing mRNA-based vaccines and therapies.

4. Experimental Section

Chemicals: Porcine gelatin was purchased from Sigma–Aldrich. PEGs of average molecular weight 2 000, 4 000, 6 000, 8 000, 10 000 and 20 000 g mol^{-1} (abbreviated as, e.g., PEG 2 000 etc.) were supplied by Sigma–Aldrich and used as received. The water used was double distilled, passed across a reverse osmosis system, and further treated with a Milli-Q plus 185 water purification apparatus. O,O-dioleyl-N-[3N-(N-methylimidazolium iodide)propylene] phosphoramidate (KLN25), O,O-dioleyl-N-histamine phosphoramidate (MM27), 1,2-dimyristoyl-sn-glycero-3-phosphoethanolamine-N-[methoxy(PEG)] (DMPE-PEG) and cholesterol were purchased from Avanti Polar Lipids (Alabaster, USA). Lipofectamine Messenger Max (LFM) was purchased from Invitrogen. Lyophilized mucin from bovine submaxillary glands was purchased from Sigma–Aldrich. Phosphate-buffered saline (PBS) containing was purchased from Sigma–Aldrich.

In vitro Transcription of GFP-mRNA: Anti-reverse cap analog (ARCA)-capped RNA with a poly(A) tail coding the reporter gene GFP (Enhanced Green Fluorescent Protein) was produced by in vitro transcription using the T7 mMessage mMachine Ultra kit. The mRNA concentration was determined by absorbance at 260 nm; mRNA had 260:280 ratios ≥ 2 and was stored at −80 °C in small aliquots.

Determination of the Liquid–Liquid Phase Diagrams: The phase diagrams of the ternary systems composed of each PEG, gelatin, and water were determined at 40 °C. The temperature was maintained at the desired value using a windowed bath with a precision of ±0.01 °C (ME-18 V Visco-Thermostat, Julabo). For the binodal curve determination, the cloud-point method was employed. To a gelatin aqueous solution at 30 wt.%, an aqueous solution of PEG (at concentrations ranging from 40 to 50 wt % depending on the MW) was added drop by drop and under constant agitation until a cloudy mixture was identified. This point indicates that a biphasic regime was reached. Afterward, the addition of pure water drop by drop and under constant agitation was performed until the solution turned limpid. At this stage, a monophasic region was reached. Following the addition of the PEG solution or water, the ternary mixture compositions were gravimetrically determined within $\pm 10^{-4}$ g and at 25 °C.

Gellable ABS Characterization: Each PEG + gelatin + water system was prepared in a 5 mL glass vial at room temperature. To obtain gelatin microspheres, the vial was heated up until 40 °C and the solution was under constant magnetic stirring (Heidolph MR Hei-Tec Magnetic Stirrer) for 15 min at a chosen mixing speed. Following this, the vial was promptly cooled in an ice bath (4 °C) for 5 min to induce gelation under constant mixing, obtaining gelatin microspheres. While to obtain a hydrogel, the resulting cold solution was transferred into a centrifuge tube, which underwent centrifugation at 4 °C and 5 000 RPM for 15 min using a refrigerated centrifuge machine (Heraeus Multifuge X1R, Thermo Scientific). The supernatant was then removed, leaving the pellet as a gelatin-rich hydrogel.

© 2025 The Author(s). Small published by Wiley-VCH GmbH

16136829, 0, Downloaded from https://onlinelibrary.wiley.com/doi/10.1002/smll.202409527 by Universidade De Aveiro, Wiley Online Library on [24/02/2025]. See the Terms and Conditions (https://onlinelibrary.wiley.com/terms-and-conditions) on Wiley Online Library for rules of use; OA articles are governed by the applicable Creative Commons License

The size and polydispersity of gelatin microspheres were determined in ethanol (95%, v/v) to prevent gelatin from swelling in solution. Before size analysis, the samples underwent ultrasonication in an ultrasonic bath Elmasonic S300 with the sample being incubated in an ice bath to prevent overheating. The total dispersion time was 5 min, with 10 s intervals off for every 20 s of operation. For visualizing the microspheres, an inverted microscope (Axiolmager 2, Zeiss) was used, under brightfield illumination or fluorescent mode. The size of the microspheres was measured using ImageJ software with at least 100 microsphere measurements per sample. Gelation time was evaluated using the inverted tube test, following the methodology outlined elsewhere.[40] Initially, 1 mL of gellable ABS solutions were incubated for 1 h at 40 °C in 5 mL glass vials. The test was carried out using the studied PEG polymers, at the same weight percentage (wt.%) for all the systems. Subsequently, the vials were placed in an ice bath, and the sol-gel transition time was determined by horizontally inverting the vials every 30 s. The point at which the gel exhibited no flow was documented as the gelation time.

Degradation Rate: The degradation rate of the hydrogels in PBS was studied following the same preparation procedure as for the gelation time assay. First, samples of 1 mL of gellable ABS solutions were incubated for 1 h at 40 °C in 5 mL glass vials. Subsequently, the vials were placed in an ice bath until gel formation. Following this, the hydrogel mass was noted, and it was placed in the release media stirring at 37 °C at 100 RPM for 60 min. During this time, samples were removed from media at selected time points (1, 2, 5, 10, 15, 30 and 60 min). The degradation rate of the gelatin-rich hydrogel was determined by protein quantification, using the Pierce BCA Protein Assay Kit by Thermo Scientific.

Scanning Electron Microscopy: Scanning electron microscopy (SEM) was performed using a high-resolution field emission SEM (HR-FESEM) Hitachi SU70 microscope operated at an accelerating voltage of 15 kV. Samples for microscopy analysis were prepared by freeze-drying and depositing a thin carbon film immediately prior to the sample analysis to ensure sample conductivity.

Liposomes Preparation: The liposome formulation was prepared by dissolving 20 wv% O,O-dioleyl-N-[3N-(N-methylimidazolium iodide)propylene] phosphoramidate (KLN25), 40 wv% O,O-dioleyl-N-histamine phosphoramidate (MM27), 1.5 wv% 1,2-dimyristoyl-sn-glycero-3-phosphoethanolamine-N-[methoxy(PEG)] (DMPE-PEG) and 38.5 wv% cholesterol in ethanol to achieve a concentration of 21.6 mM. The liposomes were prepared using PBS, with a volume ratio of 1:3 between the ethanol phase and the aqueous phase. These two phases were mixed rapidly at a total flow rate of 12 mL mi^{-1}n using a NanoAssemblr Ignite microfluidic chip (NxGen microfluidics, Precision NanoSystems, Canada). The resulting products were dialyzed against PBS at 4 °C for 6 h using dialysis tubing with a cellulose membrane (MWCO: 12.4 kDa).

Encapsulation Efficiency: The encapsulation efficiency of mRNA in liposomes was assessed using the Ribogreen assay. Briefly, samples of lipoplex, along with mRNA concentration standards, were prepared in Tris-EDTA (TE) buffer with and without Triton X-100. These were added to a black 96-well plate, followed by the addition of Ribogreen dye, which fluoresces upon binding to RNA. Fluorescence was measured using a plate reader (λ_{ex}: 485 nm, λ_{em}: 528 nm). The percentage of mRNA encapsulation was calculated as the ratio of the average fluorescence intensity in TE buffer to the average fluorescence intensity in TE buffer with Triton X-100.

Lipoplex Preparation and Hydrogel Loading: The GFP mRNA-loaded lipoplexes were prepared by mixing GFP mRNA and liposomes in a charge ratio of 1:1.5 and leaving them to form for 15 min at room temperature. The hydrogels used in the bioassays were formulated to contain 0.1 wt.% of mRNA-loaded lipoplexes. To ensure their homogeneous distribution within the system, the preparation was carried out at 37 °C, above the gelation temperature of the biopolymer. This process facilitated the uniform entrapment of mRNA-loaded liposomes within the gelatin-rich microspheres during hydrogel formation. LFM lipoplexes were prepared following the manufacturer's instructions.

Electrophoretic Gel Retardation Assay: mRNA complexation with liposomes was monitored by electrophoresis to assess lipoplex formation and partitioning at mRNA/liposome charge ratio of 1:1.5 through 0.6% agarose gel containing 0.02% of Ribogreen (ThermoFisher, France). Naked mRNA and positive control (lipoplex) were prepared containing 200 ng of mRNA per well, while the gellable ABS was prepared containing lipoplexes with 500 ng of mRNA and then the gelatin-rich hydrogel was separated and injected into separate wells. To isolate and analyze mRNA from liposomes, a 1% v/v Triton X-100 solution in TE buffer was added to the release media liposome samples and incubated on ice. Gels were imaged using a GelDocXR+ Imager (Biorad, Hercules, CA, USA).

Preparation of Mucin Samples: To prepare a 0.5 wv% mucin solution, 50 mg of lyophilized mucin from bovine sub-maxillary glands (Merck, France) were dissolved in 10 mL of PBS. The resulting mixture was vortexed at 25 °C until the mucin was fully dissolved. The air-way mucin hydrogel was created by dissolving mucins in PBS buffer at a concentration of 2.5 wv% at 25 °C. The solution was stirred for 1 h before being used.

Cell Culture: NCI-H292 airway epithelial cells line was obtained from Professor Didier Betbeder (Vaxinano, Lille, France). The cells were cultured in Roswell Park Memorial Institute medium (RPMI 1640, Thermo Fisher Scientific) supplemented with 10% heat-inactivated fetal bovine serum (FBS), 100 U mL^{-1} penicillin, 100 mg mL^{-1} streptomycin, and 1 vv% l-glutamine (Thermo Fisher Scientific) at 37 °C in a 5% CO2 humidified atmosphere. Cells were myco-plasma-free as evidenced by MycoAlert Mycoplasma Detection Kit (Lonza, Levallois Perret, France).

Transfection and Flow Cytometry: Cells were seeded at a density of 1,2 × 10^5 cells per well in 24-well plates 24 h prior to the treatment. The cells were exposed to mucin and then treated with the lipoplex-loaded hydrogel containing 0.5 µg of GFP-mRNA per well (nanoparticle:mucin ratio of 1:5 (v/v)) in well inserts (Corning, UK). Media was replaced after 4 h with a fresh one containing 10% FBS. Transfection efficiency was evaluated at 24 h after treatment. Cells were then harvested using trypsin (Thermo Fisher Scientific), collected by centrifugation (1500 RPM, 5 min), and diluted in PBS. Just before fluorescence measurement, cells were shortly vortexed and propidium iodide (PI) was added to reach a final concentration of 0.01 mg mL^{-1}. The cell-associated fluorescence intensity was measured with a flow cytometer (FORTESSA X20; Becton Dickinson, Franklin Lakes, NJ, USA) with λ_{ex} = 488 nm; λ_{em} = 530 ± 30 nm and λ_{ex} = 537 nm; λ_{em} = 618 nm for PI. The fluorescence intensity was expressed as the mean fluorescence intensity of 10000 events.

Statistical Analysis: Data were presented as mean ± standard deviation (SD). Statistical comparisons between groups were conducted using one-way ANOVA, followed by Tukey's post-hoc test. A significance level of $p < 0.05$ was considered statistically significant for all tests. To perform the analysis of the quantitative data, the program IBM SPSS Statistics was used.

Supporting Information

Supporting Information is available from the Wiley Online Library or from the author.

Acknowledgements

This work was developed within the scope of the project CICECO – Aveiro Institute of Materials, UIDB/50011/2020 (DOI 10.54499/UIDB/50011/2020), UIDP/50011/2020 (DOI 10.54499/UIDP/50011/2020) & LA/P/0006/2020 (DOI 10.54499/LA/P/0006/2020), financed by national funds through the FCT/MCTES (PIDDAC). This work was developed within the scope of the EIC-Pathfinder YSCRIPT project with reference 101047214, supported by the budgets of the Horizon Europe Program. Bojan Kopilovic acknowledges the FCT for the PhD grant (https://doi.org/10.54499/2020.06481.BD). Nabila Laroui and Chantal Pichon are grateful to ANR France 2030 PEPR BBTI for the RNAvac funding.

Conflict of Interest

The authors declare no conflict of interest.

© 2025 The Author(s). Small published by Wiley-VCH GmbH

16136829, 0, Downloaded from https://onlinelibrary.wiley.com/doi/10.1002/smll.202409527 by Universidade De Aveiro, Wiley Online Library on [24/02/2025]. See the Terms and Conditions (https://onlinelibrary.wiley.com/terms-and-conditions) on Wiley Online Library for rules of use; OA articles are governed by the applicable Creative Commons License

Data Availability Statement

The data that support the findings of this study are available in the supplementary material of this article.

Keywords

aqueous biphasic systems, mRNA, nasal delivery, thermoresponsive

Received: October 15, 2024
Revised: December 15, 2024
Published online:

[1] A. MaHam, Z. Tang, H. Wu, J. Wang, Y. Lin, *Small* **2009**, *5*, 1706.
[2] E. C. Lavelle, R. W. Ward, *Nat. Rev. Immunol.* **2022**, *22*, 236.
[3] M. M. Billingsley, N. Gong, A. J. Mukalel, A. S. Thatte, R. El-Mayta, S. K. Patel, A. E. Metzloff, K. L. Swingle, X. Han, L. Xue, A. G. Hamilton, *Small* **2024**, *20*, 2304378.
[4] N. Pardi, M. J. Hogan, F. W. Porter, D. Weissman, *Nat. Rev. Drug Discovery* **2018**, *17*, 261.
[5] C. Bai, C. Wang, Y. Lu, *Small* **2023**, *19*, 2303713.
[6] M. Yin, H. Sun, Y. Li, J. Zhang, J. Wang, Y. Liang, K. Zhang, *Small* **2024**, *20*, 2402715.
[7] X. Wen, K. Xi, Y. Tang, J. Bian, Y. Qin, W. Xiao, W. Cui, *Small* **2023**, *19*, 2207030.
[8] U. Sahin, K. Karikó, Ö. Türeci, *Nat. Rev. Drug Discovery* **2014**, *13*, 759.
[9] P. M. Tiwari, D. Vanover, K. E. Lindsay, S. S. Bawage, J. L. Kirschman, S. Bhosle, A. W. Lifland, C. Zurla, P. J. Santangelo, *Nat. Commun.* **2018**, *9*, 3999.
[10] Y. Jiao, W. C. Huang, K. Chiem, Y. Song, J. Sun, S. K. Chothe, S. Zhou, Y. Luo, M. T. Mabrouk, J. Ortega, S. V. Kuchipudi, *Small* **2024**, *20*, 2304534.
[11] N. L. Trevaskis, L. M. Kaminskas, C. J. H. Porter, *Nat. Rev. Drug Discovery* **2015**, *14*, 781.
[12] R. Anggraeni, I. D. Ana, H. Wihadmadyatami, *Clin. Exp. Vaccine Res.* **2022**, *11*, 235.
[13] R. Zhong, S. Talebian, B. B. Mendes, G. Wallace, R. Langer, J. Conde, J. Shi, *Nat. Mater.* **2023**, *22*, 818.
[14] S. Ramachandran, S. R. Satapathy, T. Dutta, *Pharm Med* **2022**, *36*, 11.
[15] C. Pineda, G. Castañeda Hernández, I. A. Jacobs, D. F. Alvarez, C. Carini, *BioDrugs* **2016**, *30*, 195.
[16] E. J. Anderson, N. G. Rouphael, A. T. Widge, L. A. Jackson, P. C. Roberts, M. Makhene, J. D. Chappell, M. R. Denison, L. J. Stevens, A. J. Pruijssers, A. B. McDermott, *N. Engl. J. Med.* **2020**, *383*, 2427.
[17] E. A. W. Smits, J. A. Soetekouw, E. H. E. Pieters, C. J. P. Smits, N. De Wijs-Rot, H. Vromans, *Invest New Drugs* **2019**, *37*, 890.
[18] C. Gao, K. Cheng, Y. Li, R. Gong, X. Zhao, G. Nie, H. Ren, *Nano Lett.* **2022**, *22*, 8801.
[19] X. Fu, T. Chen, Y. Song, C. Feng, H. Chen, Q. Zhang, G. Chen, X. Zhu, *Small* **2021**, *17*, 2101224.
[20] M. Foox, M. Zilberman, *Expert Opinion on Drug Delivery* **2015**, *12*, 1547.
[21] G. Ben Messaoud, S. Aveic, M. Wachendoerfer, H. Fischer, W. Richtering, *Small* **2023**, *19*, 2208089.
[22] K. Schwabe, A. Ewe, C. Kohn, T. Loth, A. Aigner, M. C. Hacker, M. Schulz-Siegmund, *Int. J. Pharm.* **2017**, *526*, 178.
[23] T. Furst, G. R. Dakwar, E. Zagato, A. Lechanteur, K. Remaut, B. Evrard, K. Braeckmans, G. Piel, *J. Controlled Release* **2016**, *236*, 68.
[24] R. Chen, H. Zhang, J. Yan, J. D. Bryers, *Gene Ther.* **2018**, *25*, 556.
[25] K. Ulubayram, E. Aksu, S. I. D. Gurhan, K. Serbetci, N. Hasirci, *J. Biomater. Sci., Polym. Ed.* **2002**, *13*, 1203.
[26] S. P. M. Ventura, F. A. E. Silva, M. V. Quental, D. Mondal, M. G. Freire, J. A. P. Coutinho, *Chem. Rev.* **2017**, *117*, 6984.
[27] P. A. J. Rosa, I. F. Ferreira, A. M. Azevedo, M. R. Aires-Barros, *J. Chromatogr. A* **2010**, *1217*, 2296.
[28] C. Almeida, A. Q. Pedro, A. P. M. Tavares, M. C. Neves, M. G. Freire, *Front. Bioeng. Biotechnol.* **2023**, *11*, 1037436.
[29] A. Vila, H. Gill, O. McCallion, M. J. Alonso, *J. Controlled Release.* **2004**, *98*, 231.
[30] M.-R. Yang, Y.-T. Cheng, H.-C. Tsai, H. F. Darge, C.-C. Huang, S.-Y. Lin, *Biomaterials Advances* **2023**, *152*, 213504.
[31] J. M. Lee, E.-S. Chan, R. Nagasundara Ramanan, C. W. Ooi, *Fluid Phase Equilib.* **2020**, *508*, 112441.
[32] X. Wang, B. Partlow, J. Liu, Z. Zheng, B. Su, Y. Wang, D. L. Kaplan, *Acta Biomater.* **2015**, *12*, 51.
[33] K. Zwiorek, C. Bourquin, J. Battiany, G. Winter, S. Endres, G. Hartmann, C. Coester, *Pharm. Res.* **2008**, *25*, 551.
[34] M. Djabourov, J. Maquet, H. Theveneau, J. Leblond, P. Papon, *Brit. Poly. J.* **1985**, *17*, 169.
[35] M. F. Butler, M. Heppenstall-Butler, *Food Hydrocolloids* **2003**, *17*, 815.
[36] R. Sun, J. Shi, Y. Guo, L. Chen, *Front. Chem. China* **2009**, *4*, 222.
[37] S. Cao, L. Li, Y. Du, J. Gan, J. Wang, T. Wang, Y. Liu, W. Liu, Y. Zhou, X. Gao, H. Li, *Colloids Surf. B Biointerfaces* **2021**, *207*, 112013.
[38] C. Delehedde, I. Ciganek, N. Rameix, N. Laroui, C. Gonçalves, L. Even, P. Midoux, C. Pichon, *Int. J. Pharm.* **2023**, *647*, 123531.
[39] Y. P. Lim, A. W. Mohammad, *Food Bioprocess Technol* **2011**, *4*, 304.
[40] T. Carvalho, R. Bártolo, S. N. Pedro, B. F. Valente, R. J. Pinto, C. Vilela, M. A. Shahbazi, H. A. Santos, C. S. Freire, *ACS Appl. Mater. Interfaces* **2023**, *15*, 25860.

© 2025 The Author(s). Small published by Wiley-VCH GmbH

16136829, 0, Downloaded from https://onlinelibrary.wiley.com/doi/10.1002/smll.202409527 by Universidade De Aveiro, Wiley Online Library on [24/02/2025]. See the Terms and Conditions (https://onlinelibrary.wiley.com/terms-and-conditions) on Wiley Online Library for rules of use; OA articles are governed by the applicable Creative Commons License